Li *et al. Molecular Cancer* (2024) 23:216
https://doi.org/10.1186/s12943-024-02126-4

Molecular Cancer

CORRESPONDENCE Open Access

Deciphering the role of LGALS2: insights into tertiary lymphoid structure-associated dendritic cell activation and immunotherapeutic potential in breast cancer patients

Shuyu Li[1†], Nan Zhang[2†], Hao Zhang[3†], Zhifang Yang[1†], Quan Cheng[4,5*], Kang Wei[6*], Meng Zhou[7*] and Chenshen Huang[8*]

Abstract

Recent advances in cancer research have highlighted the pivotal role of tertiary lymphoid structures (TLSs) in modulating immune responses, particularly in breast cancer (BRCA). Here, we performed an integrated analysis of bulk transcriptome data from over 6000 BRCA samples using biological network-based computational strategies and machine learning (ML) methods, and identified LGALS2 as a key marker within TLSs. Single-cell sequencing and spatial transcriptomics uncover the role of LGALS2 in TLS-associated dendritic cells (DCs) stimulation and reveal the complexity of the tumor microenvironment (TME) at both the macro and micro levels. Elevated LGALS2 expression correlates with prolonged survival, which is associated with a robust immune response marked by diverse immune cell infiltration and active anti-tumor pathways leading to a 'hot' tumor microenvironment. The colocalization of LGALS2 with TLS-associated DCs and its role in immune activation in BRCA were confirmed by hematoxylin-eosin (HE), immunohistochemistry (IHC), and in vivo validation analyses. The identification of LGALS2 as a key factor in BRCA not only highlights its therapeutic potential in novel TLS-directed immunotherapy but also opens new avenues in patient stratification and treatment selection, ultimately improving clinical management.

†Shuyu Li, Nan Zhang, Hao Zhang and Zhifang Yang contributed equally to this work.

*Correspondence:
Quan Cheng
chengquan@csu.edu.cn
Kang Wei
weikang@whu.edu.cn
Meng Zhou
zhoumeng@wmu.edu.cn
Chenshen Huang
chenshenhuang@126.com

Full list of author information is available at the end of the article

Keywords LGALS2, Breast cancer immunotherapy, Tertiary lymphoid structures, Dendritic cell activation, Tumor microenvironment

Introduction

Breast cancer (BRCA), driven by genetic and environmental factors, is a heterogeneous disease that disrupts breast tissue cell growth, making it the leading cause of cancer-related morbidity and mortality among women worldwide [1, 2]. Despite advancements in targeted therapies, ongoing treatment failures in BRCA highlight the need for new strategies to identify and use novel therapeutic targets.

Recent research has highlighted the critical role of the tumor microenvironment (TME) in determining cancer cell fate [3]. The formation of multicellular structures like tertiary lymphoid structures (TLSs) within the TME significantly impacts tumor behavior and therapy response. TLSs are particularly effective in driving anti-tumor immunity in diseases, such as melanoma, sarcoma, and BRCA, making them as important targets for immunotherapeutic strategies [4–6]. TLSs are intricate formations predominantly comprising B cells, T cells, and dendritic cells (DCs), which infiltrate and cluster within TME at cancer sites [7]. B and T lymphocytes are central to effective anti-tumor immune responses and are often found in abundance in tumor regions where immunotherapy is most effective [8]. Activated DCs play a pivotal role in anti-tumor immunity by transporting major histocompatibility complex (MHC)-antigen complexes to T cells, thereby triggering antigen-specific T cell expansion and activation [9]. Unraveling the role of DCs in antigen presentation within TLSs is critical for advancing cancer therapy. Although TLSs are recognized as potential immunotherapy markers, the exact mechanisms of their function, especially the role of DCs in BRCA, need to be further explored. Elucidation of these mechanisms could unveil new immunotherapy targets and improve patient outcomes.

In this study, a comprehensive four-step large-scale bulk RNA-seq analysis was conducted by integrating with biological network-based computational strategies and machine learning (ML) methods. Integrative bulk transcriptomic analysis, which involved molecular subtyping, key co-expression network modules, molecular interactions network with prior knowledge, and classification and survival dimensionality reduction, identified LGALS2 as a critical TLS marker and prognostic factor in BRCA. Furthermore, in-depth scRNA-seq and stRNA-seq coupled with experimental validation revealed the role of LGALS2 in activating TLS-associated DCs, creating new opportunities to improve immunotherapy effectiveness in BRCA patients.

Results

A comprehension of the genes connected to TLS molecular subtyping

BRCA patients were subtyped into two clusters, C1 and C2, using PAM and nine TLS-specific genes, with C1 comprising 470 cases and C2 comprising 614 cases, in the TCGA dataset. C1 exhibited significantly higher expression of TLS-specific genes and notable differences included: (1) enhanced ImmPort pathway activities such as antigen presentation, and TCR and BCR signaling; (2) increased immune infiltration of T cells, B cells, and DCs; and (3) greater expression of immune checkpoints such as PD-1, PD-L1, and CTLA-4 (Fig. 1A). UMAP analysis clearly separated the clusters (Figure S1A) and showed prolonged overall survival in C1 (Figure S1B). Expression of TLS-specific genes was notably higher in C1 (Figure S1C), and enrichment analysis of upregulated DEGs in C1 identified activation of immunological pathways related to cytokines, chemokines, and interferons (Figure S1D). Six ML algorithms for classification, including Pamr, RF, SVM, LassoLR, XGBoost, and Boruta, identified ten intersecting genes critical for TLS subtyping (Fig. 1B).

WGCNA discerning the TLS-attached gene module

Using WGCNA and the ssGSEA algorithm based on nine TLS-specific genes, ten gene modules were discovered, with the brown gene module being identified as having the highest correlation ($R=0.69$) with TLS, as shown in Fig. 1C. The brown module exhibited a high correlation ($R=0.82$) between module membership and gene significance for TLS (Fig. 1D). This study also linked the brown module to PROGENy-based oncological pathways such as JAK-STAT, NF-κB, TNF-α, and TRAIL, showing strong positive correlations with TLS (Figure S2A). Gene characteristics within the brown module were further detailed, including expression levels and interactions (Figure S2B).

Topology-based filtering of genes dependent on TLS by PPIRWR

The PPIRWR procedure for determining the TLS-associated gene ranking is shown in Fig. 1E. Using the gene ranking vector, GSEA assessed KEGG oncological (Figure S3A) and immunological (Figure S3B) pathways, highlighting enrichment in pathways such as BRCA, P53/TGF-β, and PD-L1/PD-1 checkpoints. A significant correlation was found among nine immunotherapeutic signatures, including CYT, IFNγIS, AyersExpIS, GEP, RohIS, DavoliIS, chemokineIS, RIR, and ImmuneScore,

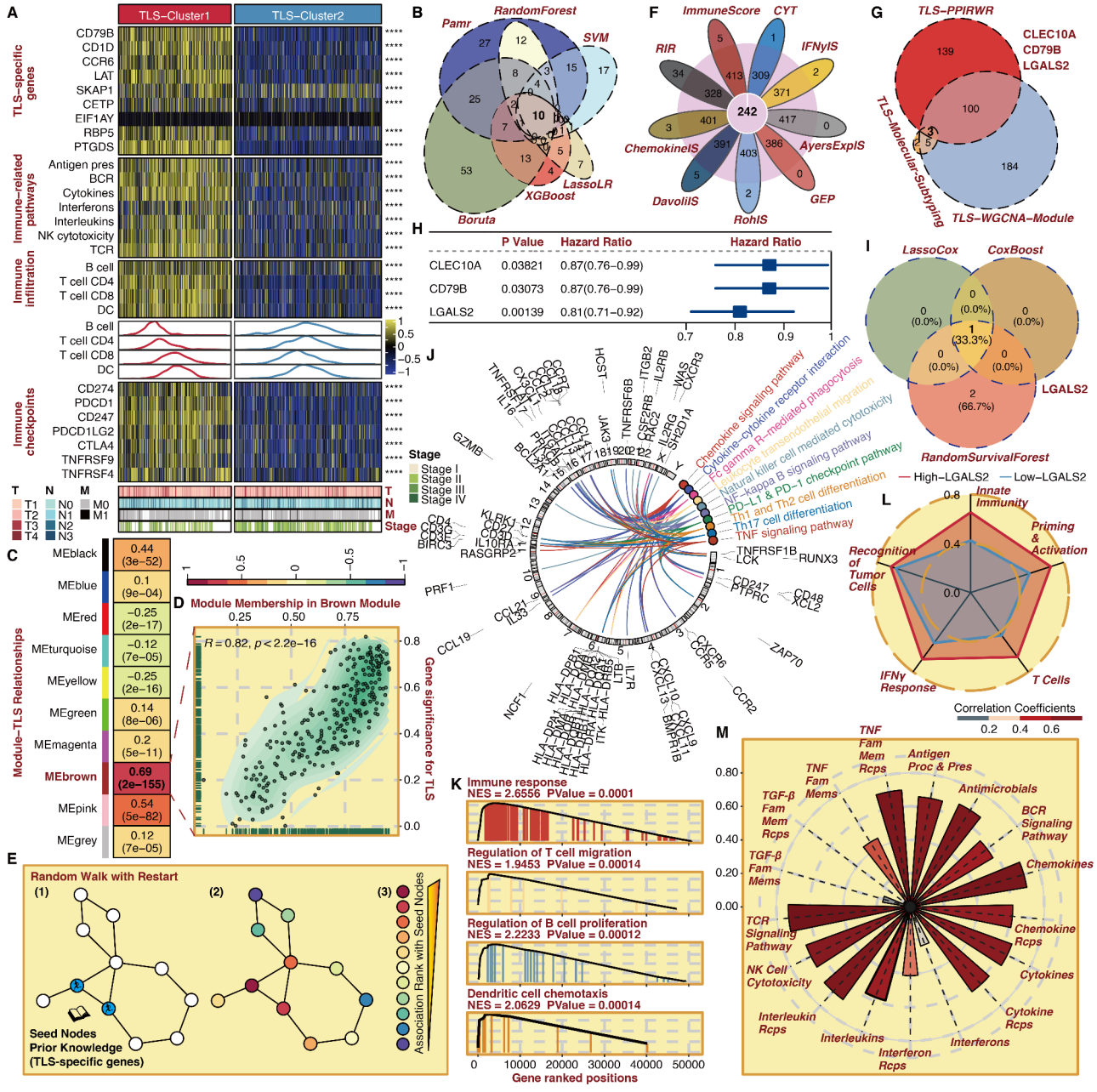

Fig. 1 Identification of TLS-associated tumor suppressor LGALS2

(**A**) Heatmap showed the distribution of nine TLS-specific genes, ImmPort-based immune-related pathways, TIMER-based immune cells, and immune checkpoints in two TLS-related clusters. (**B**) Venn plot showed the intersected genes among the DEGs between two TLS-related clusters optimized by six ML algorithms for classification. (**C**) Heatmap showed the relationships between gene modules and TLS phenotype. (**D**) Correlation plot showed the brown module's correlation between module membership and gene significance for TLS. (**E**) PPIRWR procedure for determining the TLS-associated gene ranking. (**F**) Petal chart showed the intersected genes that were significantly positively associated with each of the nine immunotherapeutic signatures from the top 10% of the TLS-associated gene ranking according to PPIRWR. (**G**) Venn plot showed the three intersected best genes in the context of TLS through molecular subtyping, WGCNA, and PPIRWR. (**H**) The univariate Cox regression analysis on the three intersected best TLS-related genes. (**I**) Venn plot showed the intersected gene LGALS2 was the final emerging gene among the three genes with associations with TLS by three ML algorithms for survival. (**J**) Circos plot showed the KEGG pathways correlated with LGALS2 and the distribution of genes enriched in pathways in human chromosomes. (**K**) GSEA-based GO immunological pathways for LGALS2. (**L**) Radar plot showed the correlation between LGALS2 and cancer immunogram traits. (**M**) Bar plot showed the correlation between LGALS2 and ImmPort-based immunological pathways

demonstrating their reliability for predicting immunotherapeutic responses, as shown in Figure S3C. From the top 10% of PPIRWR-ranked genes, 242 were selected as the final PPIRWR TLS-associated genes, that positively correlated with each immunotherapeutic signature (Fig. 1F).

TLS-associated tumor suppressor LGALS2 identified

CLEC10A, CD79B, and LGALS2 were identified as significant in the context of TLS through molecular subtyping, WGCNA, and PPIRWR (Fig. 1G). Univariate Cox regression analysis confirmed their significance (Fig. 1H). Then three ML algorithms for survival were applied. LassoCox optimized LGALS2 alone (Figure S4A), while CoxBoost and RSF evaluated all three genes (Figures S4B and S4C), solidifying LGALS2 as a significant protective prognostic gene (Fig. 1I and S4D). High LGALS2 expression correlated with prolonged survival in several independent datasets including METABRIC, GSE10309, and GSE96058 in GEO (Fig. 2A), with declining expression at advanced tumor stages indicating its tumor-suppressing nature (Figure S4E).

LGALS2 biological functional annotation

KEGG enrichment analysis strongly associated many important immunological pathways, including cytokine and chemokine signaling, T and NK cell activities, and checkpoints, with LGALS2 (Fig. 1J). GSEA-GO highlighted the involvement of LGALS2 in enhancing immunological processes related to T cells, B cells, DC, and IFNγ signaling (Fig. 1K and S5A). LGALS2-associated DEGs showed close ties to adaptive immune response and leukocyte activation based on Metascape (Figure S5B). High LGALS2 expression in BRCA patients also upregulated immunogram traits (Fig. 1L). The correlation of LGALS2 with ImmPort pathways was remarkable (Fig. 1M). The distribution patterns of Fges in five major categories and 12 minor categories suggested that LGALS2 significantly enhances immunity (Figures S5C and S5D).

Immunological features of LGALS2

Analysis of the role of LGALS2 in the BRCA cancer immune cycle revealed that it enhances several antitumor immune steps (Figure S6A). High LGALS2 expression in BRCA patients correlates with enriched immune cells such as B cells, various T cells, and activated DCs, indicating its key role in the immune microenvironment according to ESTIMATE, MCPcounter, Pornpimol-ssGSEA, and TIMER (Fig. 2B). Moreover, its interaction with immunomodulators (Figure S6B) and alignment with immunotherapeutic signatures (Fig. 2C) underscores LGALS2's potential as an effective immunotherapeutic biomarker.

Positions of LGALS2 in the microenvironment at the scRNA-seq and stRNA-seq level

From Fig. 2D, the 17 primary cell types were classified in the scRNA-seq of BRCA. LGALS2's expression patterns, as shown in Fig. 2E, showed high levels in myeloid cells, especially DCs which had the highest expression (Fig. 2F). This led to LGALS2 being identified as a DC marker, which was also confirmed by the scRNA-seq data of HCC (Figure S7A) and NSCLC (Figure S7B). The stRNA-seq of BRCA revealed that DC enrichment scores align with the expression patterns and spatial distribution of LGALS2 (Figure S7C and S7D). It was also confirmed by its strong association with the DC marker CD86 in DCs (Fig. 2G). We explored whether LGALS2 serves as a mature DC marker, noting increased LGALS2 activity over pseudo-time (Fig. 2H-J). CytoTRACE analysis showed a negative correlation between LGALS2 and DC differentiation potential, establishing its effectiveness as a mature DC marker (Fig. 2K). Moreover, mature DCs with LGALS2 showed enhanced interactions with CD8+T cells compared to their immature counterparts (Fig. 2L). Functional analysis via GO and AUCell revealed that DCs with high LGALS2 levels resemble mature DCs, involved in key immune processes related to DCs (Fig. 2M).

Co-localization of LGALS2 and TLS-associated DCs

TLS distribution in BRCA samples was assessed using HE staining to identify lymphoid structures. Subsequent IHC staining targeted CD20 for B cells and CD3 for T cells in serial sections, mapping their proximity within TLSs. Additional IHC staining for CD86 and LGALS2 on consecutive sections highlighted the colocalization of LGALS2 with TLS-associated DCs, suggesting LGALS2's role in DC-mediated immune responses in TLSs. Interestingly, LGALS2 showed low expression in tumor cells surrounded with TLSs, consistent with the findings in the scRNA-seq analysis (Figure S8).

In vivo validation of LGALS2

In vivo validation was performed to elucidate the immunoregulatory roles of LGALS2 in BRCA. The mRNA and protein expression of LGALS2 was significantly reduced in primary mouse DCs in the sh-LGALS2 group (Figures S9A and S9B). The tumor weight (Figures S9C and S9D) and volume (Figures S9C and S9E) were significantly increased in the C57BL/6 mice with an injection of LGALS2-suppressed DCs. Besides, the proportion of CD3+CD4+ (Figure S9F), CD3+CD8+ (Figure S9G), and CD8+IFNγ+ (Figure S9H) was significantly reduced in the sh-LGALS2 group (Figure S9J), while CD8+PD-1+ (Figure S9I) T cells was significantly increased in the sh-LGALS2 group (Figure S9J).

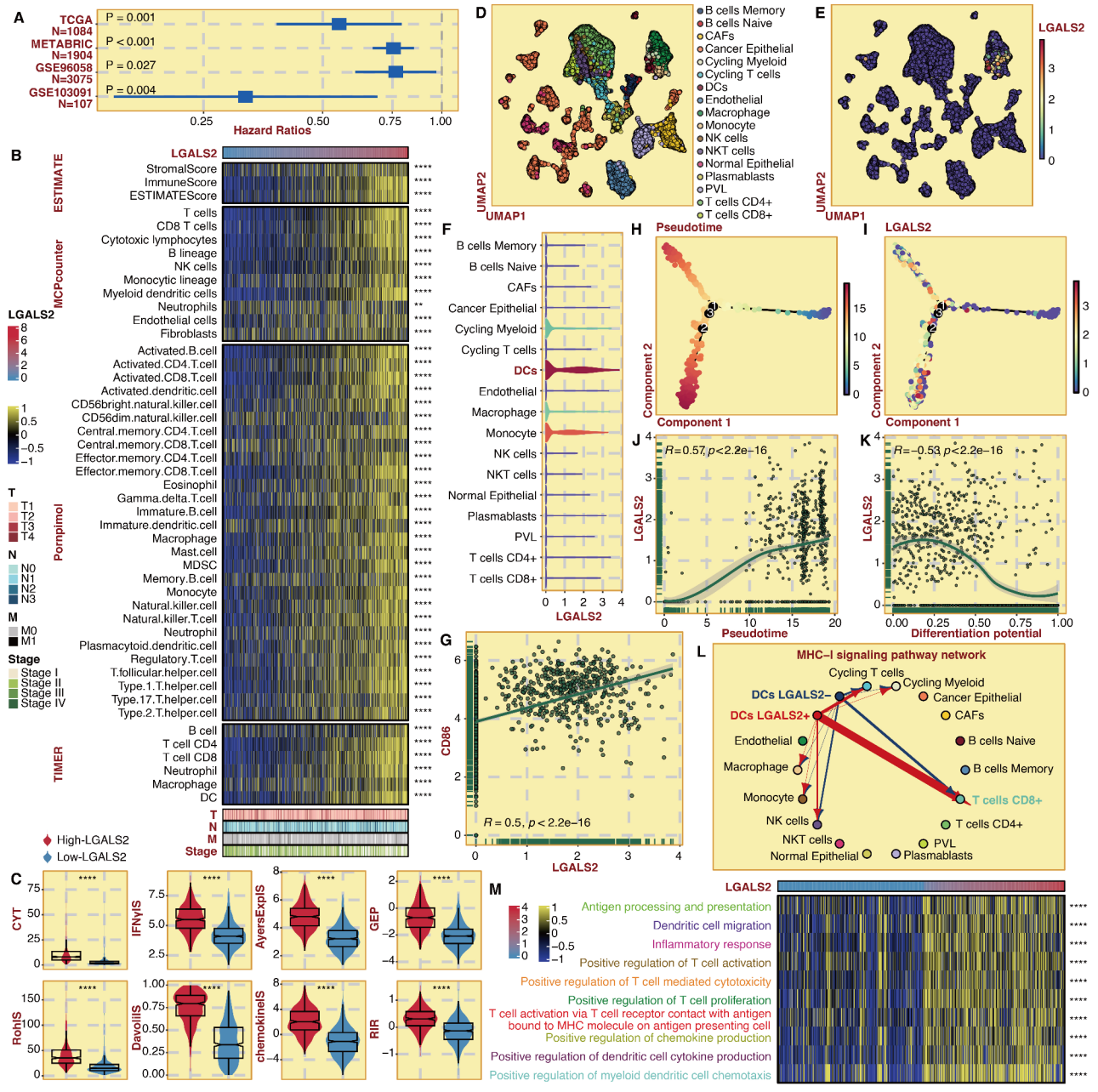

Fig. 2 Immunological features of LGALS2

(**A**) The univariate Cox regression analysis on LGALS2 in four independent BRCA datasets. (**B**) Heatmap showed the correlation between LGALS2 and infiltration of immune cells according to ESTIMATE, MCPcounter, Pornpimol-ssGSEA, and TIMER. (**C**) Box plot showed the levels of the nine immunotherapeutic signatures in two LGALS2-stratified groups. (**D**) UMAP plot showed the distribution of 17 microenvironment cell types. (**E**) UMAP plot showed the expression pattern of LGALS2 in 17 microenvironment cell types. (**F**) Violin plot showed the expression pattern of LGALS2 in 17 microenvironment cell types. (**G**) Correlation plot showed the correlation between LGALS2 and CD86 in DCs. (**H**) The reconstruction of the pseudo-time trajectory of DCs. (**I**) The expression pattern of LGALS2 in the pseudo-time trajectory of DCs. (**J**) The correlation between LGALS2 and the pseudo-time of DCs. (**K**) The correlation between LGALS2 and the differentiation potential of DCs. (**L**) The cell communication pattern of LGALS2 + and LGALS2- DCs in terms of the MHC-I signaling pathway. (**M**) Heatmap showed the correlation between LGALS2 and GO immunological pathways

Discussion

LGALS2 has been previously reported to be a prognostic marker in human breast cancer [10]. Besides, LGALS2 was identified to be an immunotherapy target in TNBC [11] and related to drug resistance [12]. Our research demonstrates that LGALS2 is not only a biomarker of BRCA but also a functional player in the immune landscape, specifically as a DC marker. Elevated LGALS2 expression correlates with increased immune cell infiltration, particularly of DCs and T cells, which are pivotal

for orchestrating anti-tumor immunity. Notably, previous studies indicated a dual role of LGALS2 in regulating T cells. LGALS2 on DCs not only regulates T cell priming and activation [13] but also induces T cell apoptosis [14]. Our in vivo validation supported its immunological enhancement role. The identification of LGALS2 as a key factor in DC activation within TLSs highlights its potential as a therapeutic target which is consistent with previous studies highlighting the importance of TLSs in promoting effective immune responses against tumors.

Abbreviations

AyersExpIS	Expanded Immune Signature
BRCA	Breast Cancer
BCR	B Cell Receptor
chemokineIS	Chemokine Immune Signature
CYT	Cytolytic Activity
DavoliIS	Davoli immune signature
DC	Dendritic Cell
DEG	Differentially Expressed Gene
ESTIMATE	Estimation of STromal and Immune cells in MAlignant Tumors using Expression data
Fges	Functional Gene Expression Signature
GEO	Gene Expression Omnibus
GEP	T Cell–Inflamed Signature
GSEA	Gene Set Enrichment Analysis
GO	Gene Ontology
HCC	Hepatocellular Carcinoma
HE	Hematoxylin-Eosin
IHC	Immunohistochemistry
ImmPort	Immunology Database and Analysis Portal
IFNγIS	Interferon-Gamma Immune Signature
JAK-STAT	Janus Kinase-Signal Transducer and Activator of Transcription
KEGG	Kyoto Encyclopedia of Genes and Genomes
LassoCox	Least Absolute Shrinkage and Selection Operator Regularized Cox Regression
LassoLR	Least Absolute Shrinkage and Selection Operator Regularized Logistic Regression
METABRIC	Molecular Taxonomy of Breast Cancer International Consortium
MCPcounter	Microenvironment Cell Population-Counter
MHC	Major Histocompatibility Complex
ML	Machine Learning
NF-κB	Nuclear Factor Kappa
NK	Natural Killer
NSCLC	Non-Small Cell Lung Cancer
Pamr	Prediction Analysis for Microarrays
PAM	Partitioning Around Medoids
PPIRWR	Protein-Protein Interaction Random Walk with Restart
PROGENy	Pathway RespOnsive GENes
RF	Random Forest
RIR	Repressed Immune Resistance
RohIS	Roh Immune Sccore
RSF	Random Survival Forest
scRNA-seq	Single-Cell RNA Sequencing
ssGSEA	Single Sample Gene Set Enrichment Analysis
stRNA-seq	Spatial Transcriptomics RNA Sequencing
SVM	Support Vector Machine
TCGA	The Cancer Genome Atlas
TCR	T Cell Receptor
TGF	Transforming Growth Factor
TIMER	Tumor Immune Estimation Resource
TLS	Tertiary Lymphoid Structure
TME	Tumor Microenvironment
TNF	Tumor Necrosis Factor
TRAIL	TNF-Related Apoptosis-Inducing Ligand
UMAP	Uniform Manifold Approximation and Projection
WGCNA	Weighted Gene Co-Expression Network Analysis

Supplementary Information

The online version contains supplementary material available at https://doi.org/10.1186/s12943-024-02126-4.

Supplementary Material 1

Acknowledgements
The authors express gratitude to the public databases, websites, and software used in this study.

Author contributions
CH, MZ, KW, and QC conceived and designed the study. NZ and SL performed the data analysis. NZ and HZ wrote the manuscript. KW and SL performed animal experiments. CH, MZ, KW, QC, and ZY revised and supervised the manuscript. All authors read, edited, and approved the final manuscript.

Funding
None.

Data availability
No datasets were generated or analysed during the current study.

Declarations

Ethical approval and consent to participate
All procedures performed in studies involving human participants were in accordance with the ethical standards of the institutional and/or national research committee and with the 1964 Helsinki Declaration and its later amendments or comparable ethical standards. All participating subjects had signed informed consent, and the experimental protocols were approved by the Ethical Committee of Tongji Hospital (ID: TJ-IRB20210928). Animal experiments were conducted in compliance with the Ethical Committee of the Zhongnan Hospital of Wuhan University (ID: WP2024307).

Consent for publication
Not applicable.

Competing interests
The authors declare no competing interests.

Author details
[1]Department of Thyroid and Breast Surgery, Tongji Hospital, Tongji Medical College, Huazhong University of Science and Technology, Wuhan, China
[2]College of Life Science and Technology, Huazhong University of Science and Technology, Wuhan, China
[3]Department of Neurosurgery, The Second Affiliated Hospital, Chongqing Medical University, Chongqing, China
[4]Department of Neurosurgery, Xiangya Hospital, Central South University, Changsha, Hunan 410008, P. R. China
[5]National Clinical Research Center for Geriatric Disorders, Xiangya Hospital, Central South University, Changsha, China
[6]Department of Plastic Surgery, Zhongnan Hospital of Wuhan University, Wuhan, Hubei 430071, P.R. China
[7]School of Biomedical Engineering, Wenzhou Medical University, Wenzhou, Zhejiang 325027, P.R. China
[8]Department of Gastrointestinal Surgery, Fujian Provincial Hospital, Fuzhou University Affiliated Provincial Hospital, Fuzhou, Fujian 350001, P.R. China

Received: 17 May 2024 / Accepted: 17 September 2024
Published online: 30 September 2024

References

1. Majeed W, Aslam B, Javed I, Khaliq T, Muhammad F, Ali A, Raza A. Breast cancer: major risk factors and recent developments in treatment. Asian Pac J Cancer Prev. 2014;15:3353–8.

2. Harbeck N, Gnant M. Breast cancer. Lancet. 2017;389:1134–50.
3. Hinshaw DC, Shevde LA. The tumor microenvironment innately modulates cancer progression. Cancer Res. 2019;79:4557–66.
4. Cabrita R, Lauss M, Sanna A, Donia M, Skaarup Larsen M, Mitra S, Johansson I, Phung B, Harbst K, Vallon-Christersson J, van Schoiack A, Lovgren K, Warren S, Jirstrom K, Olsson H, Pietras K, Ingvar C, Isaksson K, Schadendorf D, Schmidt H, Bastholt L, Carneiro A, Wargo JA, Svane IM, Jonsson G. Tertiary lymphoid structures improve immunotherapy and survival in melanoma. Nature. 2020;577:561–5.
5. Petitprez F, de Reynies A, Keung EZ, Chen TW, Sun CM, Calderaro J, Jeng YM, Hsiao LP, Lacroix L, Bougouin A, Moreira M, Lacroix G, Natario I, Adam J, Lucchesi C, Laizet YH, Toulmonde M, Burgess MA, Bolejack V, Reinke D, Wani KM, Wang WL, Lazar AJ, Roland CL, Wargo JA, Italiano A, Sautes-Fridman C, Tawbi HA, Fridman WH. B cells are associated with survival and immunotherapy response in sarcoma. Nature. 2020;577:556–60.
6. Acar E, Esendagli G, Yazici O, Dursun A. Tumor-infiltrating lymphocytes (TIL), tertiary lymphoid structures (TLS), and expression of PD-1, TIM-3, LAG-3 on TIL in invasive and in situ ductal breast carcinomas and their relationship with prognostic factors. Clin Breast Cancer. 2022;22:e901–15.
7. Schumacher TN, Thommen DS. Tertiary lymphoid structures in cancer. Science. 2022;375:eabf9419.
8. N J, Sl TJN, Gt B. Tertiary lymphoid structures and B lymphocytes in cancer prognosis and response to immunotherapies. Oncoimmunology. 2021;10:1900508.
9. Lian J, Luster AD. Chemokine-guided cell positioning in the lymph node orchestrates the generation of adaptive immune responses. Curr Opin Cell Biol. 2015;36:1–6.
10. Chetry M, Bhandari A, Feng R, Song X, Wang P, Lin J. Overexpression of galectin2 (LGALS2) predicts a better prognosis in human breast cancer. Am J Transl Res. 2022;14:2301–16.
11. Ji P, Gong Y, Jin ML, Wu HL, Guo LW, Pei YC, Chai WJ, Jiang YZ, Liu Y, Ma XY, Di GH, Hu X, Shao ZM. In vivo multidimensional CRISPR screens identify Lgals2 as an immunotherapy target in triple-negative breast cancer. Sci Adv. 2022;8:eabl8247.
12. He S, Ji Z, Zhang Q, Zhang X, Chen J, Hu J, Wang R, Ding Y. Investigation of LGALS2 expression in the TCGA database reveals its clinical relevance in breast cancer immunotherapy and drug resistance. Sci Rep. 2023;13:17445.
13. Liu FT, Stowell SR. The role of galectins in immunity and infection. Nat Rev Immunol. 2023;23:479–94.
14. Sturm A, Lensch M, Andre S, Kaltner H, Wiedenmann B, Rosewicz S, Dignass AU, Gabius HJ. Human galectin-2: novel inducer of T cell apoptosis with distinct profile of caspase activation. J Immunol. 2004;173:3825–37.

Publisher's note